

Changes of rural to urban areas in hydrograph characteristics on watershed divisions

Jet-chau Wen, Yen-jen Lee, Shin-jen Cheng & Ju-huang Lee

Natural Hazards

Journal of the International Society
for the Prevention and Mitigation of
Natural Hazards

ISSN 0921-030X

Nat Hazards
DOI 10.1007/s11069-014-1220-6



Your article is protected by copyright and all rights are held exclusively by Springer Science +Business Media Dordrecht. This e-offprint is for personal use only and shall not be self-archived in electronic repositories. If you wish to self-archive your article, please use the accepted manuscript version for posting on your own website. You may further deposit the accepted manuscript version in any repository, provided it is only made publicly available 12 months after official publication or later and provided acknowledgement is given to the original source of publication and a link is inserted to the published article on Springer's website. The link must be accompanied by the following text: "The final publication is available at link.springer.com".

Changes of rural to urban areas in hydrograph characteristics on watershed divisions

Jet-chau Wen · Yen-jen Lee · Shin-jen Cheng · Ju-huang Lee

Received: 12 January 2014 / Accepted: 3 May 2014
© Springer Science+Business Media Dordrecht 2014

Abstract This study examined changes in hydrograph characteristics of rural statuses to urban statuses on watershed divisions in Taiwan. The main approach was to relate applicable model parameters with the corresponding imperviousness based on calibration and verification using a semidistributed model and 102 events. The model structure is conceptual linear reservoirs with parallel-type cascaded storages which is represented by overland and channel coefficients. The hourly mean rainfall of the watershed and its divisions were calculated using the Kriging method. The time-variant rainfall losses were calculated using the constant percentage method. The spatial and temporal model inputs, division effective rainfall, were obtained by subtracting mean rainfall of divisions from the rainfall losses. In calibration, the storage values of 50 events derived using appropriate parameter bounds were more reasonable than those using inappropriate bounds. Based on the optimal interval method, the overland storages displayed more marked change than did channel storage in response to imperviousness changes. By contrast, the channel storages were unaffected by the changes in urbanization. The overland storages were related with the imperviousness by using the regression equations for determining their relationships in continuous changes of urbanized divisions. The verification of the regression relationships was based on 52 events. The results indicated that power linkage was an available selection

J. Wen

Department of Safety Health and Environmental Engineering, National Yunlin University of Science and Technology, Douliou, Yunlin 640, Taiwan

Y. Lee

Graduate School of Engineering Science and Technology, National Yunlin University of Science and Technology, Douliou, Yunlin 640, Taiwan

S. Cheng (✉)

Department of Leisure and Recreation Management, Taiwan Shoufu University, 168, Nan-shih Li, Madou, Tainan 721, Taiwan
e-mail: sjcheng@tsu.edu.tw

J. Lee

Water Resources Agency, Ministry of Economic Affairs, Taipei 106, Taiwan

for linking division parameters with the corresponding imperviousness. Finally, the study concludes (1) appropriate bounds in parameter calibration are useful for obtaining significant storage values and (2) the study results using these suitable storages indicated large changes in imperviousness on the downstream divisions, marked urbanization resulted in reduced the time to peak at least 10 %, the peak discharge exceeded an increment of 20–30 %.

Keywords Block Kriging · Watershed divisions · Parameter bounds · Semidistributed model · Hydrograph characteristics

1 Introduction

From the time humans first inhabited the earth, they began to cluster in certain areas. Urban areas are human societies or cities by definition, the areas contained increasingly concentrated populations. During the urban development process, people moved out of rural districts and concentrated in big cities for pursuing a higher quality of life. The activity increased constructions in certain areas including schools, railroad lines, streets, roofs, parking lots, shopping malls, waterways, highways, and commercial and industrial buildings. These sophisticated environments comprised numerous impervious surfaces that were built in populated areas. The population and imperviousness may thus be available indices of the degree of urbanization in an area. The imperviousness and population variations derived from urban development are generally scattered over a watershed and are typically nonuniform distributions on a two-dimensional surface. An obvious difference should exist between a rural/upstream mountain area and an urban/downstream plain in Taiwan.

The consequence of urbanization involving increased and concentrated populations make that the amount of impervious surface in a geographical area is extended and increased. The changed imperviousness altered the infiltration mechanism of the earth's surface in the hydrological cycle (Lee and Heaney 2003; Yang and Liu 2005; Cheng et al. 2008b, 2010). An Outlet-runoff hydrograph is a composite representation of hydrological and geomorphic characteristics of a watershed responded to rainfall inputs. Although hydrograph modeling is not an only methodology (Olivera and DeFee 2007), the imperviousness index is crucial in evaluating urbanization effects using hydrological models (Cheng and Wang 2002; Huang et al. 2008a; Cheng et al. 2010). The hydrograph shape is a convenient evaluation target for exploring changes in watershed responses resulting from imperviousness changes (Singh 1998; Aronica and Cannarozzo 2000; Legesse et al. 2003; Hagg et al. 2007; Barron et al. 2013). The outlet-hydrograph shape of a developed watershed should vary with different degrees of urbanization (Kliment and Matoušková 2009), which can be represented by time and flow characteristics. These altered characteristics, which have been frequently used to understand concrete coverage of urbanization changes, include rainwater loss (Gremillion et al. 2000; Cheng et al. 2008b); surface runoff (Bonta et al. 1997; Junil et al. 1999; Rodriguez et al. 2003), runoff volume (Arnell 1982), peak discharge (Huang et al. 2008a, b), time to peak (Huang et al. 2012), storm water quality (Liu et al. 2012), and base flow (Simmons and Reynolds 1982). The combination of these effects leads to the occurrence of more serious natural disasters in various areas than those that occurred in the past.

Urbanization changes are typically spatial and temporal variations, which bring their hydrological effects varying in time period and have different influences on the upstream and downstream areas of a basin. The difficulties of exploring the hydrological effects of urbanization changes in time and space involve managing the hydrological data having spatiotemporal nature and urbanization indices with spatial and temporal variations, and hydrograph simulations of watershed divisions. Simply for unit hydrograph (UH)-based lumped modeling using the Nash (Nash 1957; Nash and Sutcliffe 1970) or Clarke (Clarke 1973; Ahmad et al. 2009) models. By way of neglecting distribution changes in the space dimension, these models calibrated suitable storage parameters for simulating direct runoff hydrographs. The instantaneous unit hydrograph (IUH) governed by parameter values can be easily used to explore the urbanization changes occurred before and after or continual change in time (Huang et al. 2008b, 2012; Cheng 2011b). Other available models possessing similar IUH forms include the IHACRES model (Jakeman et al. 1990; Jakeman and Hornberger 1993), a model of three serial linear reservoirs (Cheng 2010a, b, c), and a linear cascade model of three serial reservoirs with a parallel reservoir (Yue and Hashino 2000; Li et al. 2012; Cheng et al. 2013).

The hydrological effects of urban changes may be particularly severe in specific watershed divisions that are vulnerable to the destruction of links in the hydrological cycle. Such variations in vulnerability result from spatial changes in the movement of people and are accompanied by varying degrees of impervious paving. However, small spatial variations in local areas can be ignored by appropriately dividing the entire watershed into several divisions to reflect large spatial differences within the system. These divided watershed divisions are considered to be lumped, and linking these lumped system models together produces a model of the entire system (Hsieh and Wang 1999; Agirre et al. 2005). This study used a semidistributed parallel-type model, which is represented by overland and channel storage constants k_o and k_c , to describe the storm waters of a watershed and its divisions. The block Kriging technology was used to estimate mean rainfalls in the watershed and its divisions. The time-variant losses with a spatially constant rate were calculated using the constant percentage method (Kang et al. 1998) based on the mean rainfall and direct runoffs of events that occur in the entire watershed. The effective rainfalls in watershed divisions are derived from the mathematical differences between the mean rainfall of divisions and the constant percentage computations. The calibrated division parameters were then applied to further evaluate changes in hydrograph characteristics of watershed divisions which transformed from rural areas to an urban statuses.

2 Methods

2.1 Block Kriging

Mean rainfall is generally calculated using data obtained from raingauge sites located on a watershed, and using traditional methods such as the Thiessen polygon method. The estimator Z_K^* is typically calculated by employing a linear combination of n raingauge observations $Z(x_i)$ located at raingauge x_i and with weighting of raingauge λ_i , as follows:

$$Z_K^* = \sum_{i=1}^n \lambda_i Z(x_i) \quad (1)$$

The block Kriging method and its variants (Xie et al. 2011) also use a linear formula, as in Eq. (1), to obtain point or areal estimations of rainfall for a region. The Kriging method has numerous applications in various research fields. Typical cases include raingauge network design (Bastin et al. 1984; Cheng et al. 2008a), raingauge evaluation (Cheng 2011a; Cheng et al. 2012), the spatial interpolation of rainfall (Goovaerts 2000; Syed et al. 2003; Basistha et al. 2008), and space–time rainfall interpolation (Cheng et al. 2007). The primary difference between the Kriging method and traditional methods is the computation of raingauge weightings. The Kriging method applies the spatial relationship among rainfall variances in a two-dimensional surface, such as a semivariogram $\gamma(t, h_{ij})$ (Lebel and Bastin 1985), to calculate the weighting values of raingauges:

$$\gamma(t, h_{ij}) = \frac{1}{2T} \sum_{t=1}^T \left\{ [p(t, x_i) - p(t, x_j)]^2 \right\} \tag{2}$$

where h_{ij} represents the distance between arbitrary raingauges x_i and x_j ; T denotes the total duration of all rainfall events; and $p(t, x_i)$ defines a rainfall depth measured using the i -th raingauge at the t -th time period.

The raingauge weightings can be calculated using the block Kriging system with a given semivariogram of rainfall. The point or areal rainfall estimations are subsequently obtained using Eq. (1). The Kriging system is derived by applying the Lagrange multiplier method and Eqs. (3) and (4):

$$\begin{cases} \sum_{j=1}^n \lambda_j \gamma(x_i, x_j) + \mu = \bar{\gamma}(V, x_i), & i = 1, 2, \dots, n \\ \sum_{i=1}^n \lambda_i = 1 \end{cases} \tag{3}$$

$$\sigma_K^2 = \sum_{i=1}^n \lambda_i \bar{\gamma}(V, x_i) + \mu \tag{4}$$

where $\gamma(x_i, x_j)$ is the semivariogram of raingauges x_i and raingauge x_j ; $\bar{\gamma}(V, x_i)$ represents the mean semivariogram of the estimated area V and raingauge x_i ; λ_j is the weighting of each raingauge; σ_K^2 is the Kriging estimated variance; and μ is the Lagrange multiplier.

The semivariogram $\gamma(t, h_{ij})$ calculated using Eq. (2) cannot be used directly in the block Kriging system because it is not spatially continuous. A realistic application of the block Kriging method involves using a semivariogram model to obtain the spatial continuity of rainfall variations. Bastin et al. (1984) proposed a basic semivariogram for rapidly computing an hourly semivariogram with a continuous form. This calculation result is referred to as the scaled climatological mean semivariogram, represented by $\gamma_d^*(h_{ij}, a)$. This approach involves establishing an hourly semivariogram $\gamma(t, h_{ij})$ using dimensionless rainfall data from a project basin. The expression for Eq. (5) indicates the relationship between the hourly semivariogram and the scaled climatological mean semivariogram:

$$\gamma(t, h_{ij}) = \omega(t) \gamma_d^*(h_{ij}, a) = s^2(t) \gamma_d^*(h_{ij}, a) \tag{5}$$

where $\omega(t)$ denotes the sill of the semivariogram for period t and is time variant; a represents the range of the scaled climatological mean semivariogram and is time invariant; and $s(t)$ denotes the standard deviation of rainfall for all raingauges for period t . The basic semivariogram is expressed as

$$\gamma_d^*(h_{ij}, a) = \frac{1}{2T} \sum_{t=1}^T \left\{ \left[\frac{p(t, x_i) - p(t, x_j)}{s(t)} \right]^2 \right\} \tag{6}$$

A scaled climatological mean semivariogram with a discrete form can be calculated using Eq. (6). This basic experimental semivariogram uses a semivariogram model, such as the power model (Isaaks and Srivastava 1989), to obtain the basic semivariogram that includes the spatial continuity of rainfall variations. By applying Eq. (5), the hourly semivariograms $\gamma(t, h_{ij})$ can be easily obtained by using the basic semivariogram $\gamma_d^*(h_{ij}, a)$ and the variance of rainfall observations for all of the raingauges $s^2(t)$ for a period t .

When applying the block Kriging method to estimate the hourly mean rainfall during storm events in watershed divisions, the estimated area V in Eq. (3) must be divided into M grids. Therefore, the expression $\bar{\gamma}(V, x_i)$ in Eqs. (3) and (4) was replaced by the following equation:

$$\bar{\gamma}(V, x_i) = \frac{1}{M} \sum_{m=1}^M \gamma(V_m, x_i) \tag{7}$$

where V_m is the m -th grid of the estimated area V and $\gamma(V_m, x_i)$ represents the semivariogram of the m -th grid V_m and rain gauge x_i . Figure 1 shows the computation procedure of the mean semivariogram $\sum_{m=1}^M \gamma(V_m, x_i)/M$.

2.2 Semidistributed model of parallel-type linear reservoir cascaded storages

In hydrological modeling, a watershed response is frequently imaged as multi-reservoirs cascaded. Conceptual reservoir storages are typically used to represent a hydrological response, in which a hyetograph is transformed into a runoff hydrograph at a watershed outlet. The general form of the IUH U_n from the n -th linear cascaded reservoir possessing various storage constants k_n and period t can be derived as follows (Hsieh and Wang 1999):

$$U_n(t) = \int_0^t U_{n-1}(\tau) \frac{1}{k_n} e^{-\frac{t-\tau}{k_n}} d\tau$$

$$= \begin{cases} \frac{1}{k_1} e^{-\frac{t}{k_1}}, & n = 1 \\ \sum_{i=1}^n \frac{k_i^{n-2}}{\prod_{j=1, j \neq i}^n (k_i - k_j)} e^{-\frac{t}{k_i}}, & n \geq 2 \end{cases} \tag{8}$$

A lumped watershed system containing identical values for linear reservoir storage is the Nash model (Nash 1957) which is a special case of Eq. (8).

In this study, each watershed division was treated as an independent subsystem. The hydrological status of each subsystem was indicated by two storage parameters, the overland storage k_o and the channel storage k_c . A connection from a watershed division to the watershed outlet was constructed using a flow path. A watershed was divided into n subsystems (the number of the most upstream division is 1 and that of the outlet subsystem is n); thus, n parallel flow paths were drawn to route the outflow hydrograph at a watershed outlet. The i -th flow path resulted from the overland and channel storage of the i -th division and the channel storage of its downstream divisions at the watershed outlet. Therefore, the flow paths derived from the n divisions and their downstream channels at the watershed outlet were generally expressed as follows

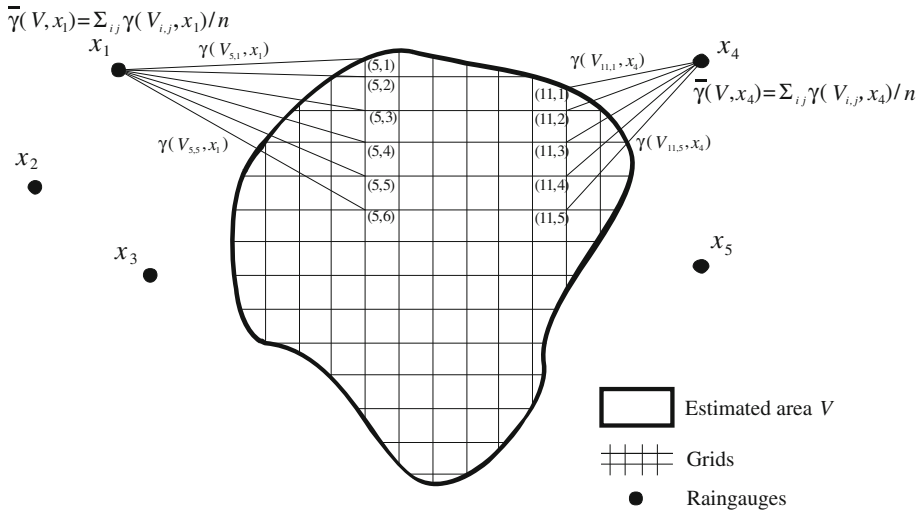


Fig. 1 Computation of the mean semivariogram between the estimated area and raingauges

$$o_i \rightarrow c_i \rightarrow c_{i+1} \rightarrow \dots \rightarrow c_{n-1} \rightarrow c_n, \quad i = 1, 2, \dots, n \tag{9}$$

where the symbol o_i denotes the overland storage of the i -th watershed division and the symbol c_i represents the channel storage of the i -th division. The maximal value of the subscript i is equal to n .

The Wu-Tu watershed was divided into four divisions; thus, four parallel flow paths/IUHs were determined to route the outflow hydrograph at an outlet of the Wu-Tu watershed. For example, the IUH $U_4(t)$ form of flow path 4 derived from Eqs (8) and (9) was determined as follows:

$$U_4(t) = \frac{1}{(Ko_4 - Kc_4)} e^{-\frac{t}{Kc_4}} + \frac{1}{(Kc_4 - Ko_4)} e^{-\frac{t}{Ko_4}} \tag{10}$$

The total direct runoff at the watershed outlet can be computed using the convolution integral, in which the spatially averaged effective rainfall $I_i(\tau)$ of each flow path is operated using IUH $U_i(t - \tau)$ and integrated over time t to yield the outlet runoff $Q(t)$. The convolution integral formula is as follows:

$$Q(t) = \sum_{i=1}^n \int_0^t I_i(\tau) U_i(t - \tau) d\tau \tag{11}$$

where the function $U_i(t - \tau)$ is the IUH derived from Eq. (8), representing the i -th flow path. The symbol n is the number of divisions in the watershed, set as $n = 4$ in this study.

3 Evaluation criteria

To measure the suitability of the model parameters for the basin of interest, the following four criteria were used to analyze the goodness of fit:

1. The *CE* was defined as

$$CE = 1 - \frac{\sum_{t=1}^T [Q_{est}(t) - Q_{obs}(t)]^2}{\sum_{t=1}^T [Q_{obs}(t) - \bar{Q}_{obs}]^2} \quad (12)$$

where $Q_{est}(t)$ denotes the discharge of the simulated hydrograph for period t (m^3/s), $Q_{obs}(t)$ is the discharge of the observed hydrograph for period t (m^3/s), and \bar{Q}_{obs} represents the mean discharge of the observed hydrograph (m^3/s). A *CE* value close to one indicates a good fit.

2. The $EQ_p(\%)$ was defined as

$$EQ_p(\%) = \frac{Q_{p,est} - Q_{p,obs}}{Q_{p,obs}} \times 100\% \quad (13)$$

where $Q_{p,est}$ is the peak discharge of the simulated hydrograph (m^3/s) and $Q_{p,obs}$ is the peak discharge of the observed hydrograph (m^3/s).

3. The ET_p was defined as

$$ET_p = T_{p,est} - T_{p,obs} \quad (14)$$

where $T_{p,est}$ denotes the time (h) required for the peak to occur in the simulated hydrographs and $T_{p,obs}$ represents the actual time (h) required for the peak to occur in the observed hydrographs.

4. The *VER* (%) was defined as

$$VER = \frac{\sum_{t=1}^T Q_{est}(t) - \sum_{t=1}^T Q_{obs}(t)}{\sum_{t=1}^T Q_{obs}(t)} \times 100\% \quad (15)$$

4 The study watershed

4.1 Geographical features

The Tamshui River is the third longest river in Taiwan, and one of the chief tributaries is the Kee-Lung River (Fig. 2a). The Wu-Tu watershed is located upstream of the Kee-Lung River and was chosen as the research site in this study. The selected watershed covers nearly 204 km² and surrounds Taipei City in Northern Taiwan (Fig. 2b). The mean annual precipitation and runoff depth of the entire Wu-Tu watershed are 2,865 and 2,177 mm, respectively. The watershed consists of a large pervious area (high mountains) and a smaller impervious area (watershed downstream), with most of the runoff flowing from the pervious area. The rugged topography of the watershed indicates that the runoff path lines are short and steep; in addition, rainfall is nonuniform in time and space. Large floods occur rapidly in the middle-to-downstream reaches of the watershed, causing serious damage during the summer.

4.2 Data used

Fourteen raingauges were located along the Tamshui River (Fig. 2a). Three of the raingauges (at Jui-Fang, Wu-Tu, and Huo-Shao-Liao) and one discharge site (Wu-Tu) were located within the Wu-Tu watershed (Fig. 2b). The study data comprised records for 102 rainfall-runoff events between 1966 and 2008. The degree of urbanization in the research area was gleaned from annual data on population density and imperviousness percentage. This study used the data from 50 events to calibrate the model parameters of four watershed divisions and used the remaining 52 events to test the model verification.

Two identified urbanization variables were convenient for observing the extent of urbanization, such as population density and imperviousness percentage. As shown in Fig. 3, changes in population density and imperviousness percentage were plotted for the Wu-Tu watershed divisions between 1966 and 2008. Figures 3c, d show the concurrently increased indices of imperviousness percentage and population density on the downstream divisions (Divisions 3 and 4) of the watershed. While the two upstream divisions (Divisions 1 and 2) exhibited distinct changes from the downstream divisions, such as a slow increase in imperviousness and a markedly decreased in the population, as shown in Fig. 3a, b. This study used one of two urbanization variables, imperviousness, as the primary reference of urbanization. The imperviousness index was used in relation to model parameters for exploring the hydrological consequences of urbanization in the Wu-Tu watershed divisions. In impervious paving, all rainfall generates surface runoff. The annual imperviousness percentage for each year was obtained based on this definition and included streets, roads, railroad lines, highways, roofs, buildings, parking lots, ponds, lakes, and waterways.

5 Results and discussions

This study investigated changes of rural to urban statuses in characteristics of division-outlet hydrographs. The hydrographs and their parameters of watershed divisions were calibrated from a semidistributed model. The proposed model was an UH-based model involving assessed parallel type, linearly multi-cascaded reservoirs with overland and channel storages, k_o and k_c . The applicable division parameters were discussed through suitable parameter bounds in calibrations for the storage parameters fit in with their physical significances themselves. The urbanization index, imperviousness, is frequently used as a variable of watershed development in hydrology. This study-related division parameters with imperviousness percentages to compare continuous variations of the hydrological status on urbanized divisions in space and time. By the way of these verified relationships, storage values can be obtained based on imperviousness changes, and characteristic changes in division hydrographs owing to each urbanization consequence were evaluated and discussed.

5.1 Effective rainfall of watershed divisions

Calculating mean rainfall is the first job for hydrological modeling. The block Kriging was used to estimate mean rainfall of the Wu-Tu watershed and its four divisions. The semi-variogram in the block Kriging must be determined in advance. The hourly semivariogram

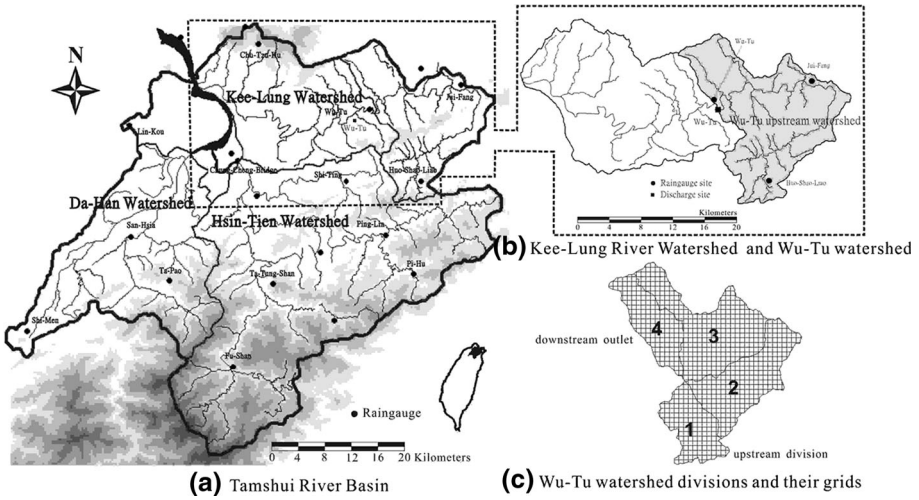


Fig. 2 Map of the Wu-Tu watershed and its four watershed divisions

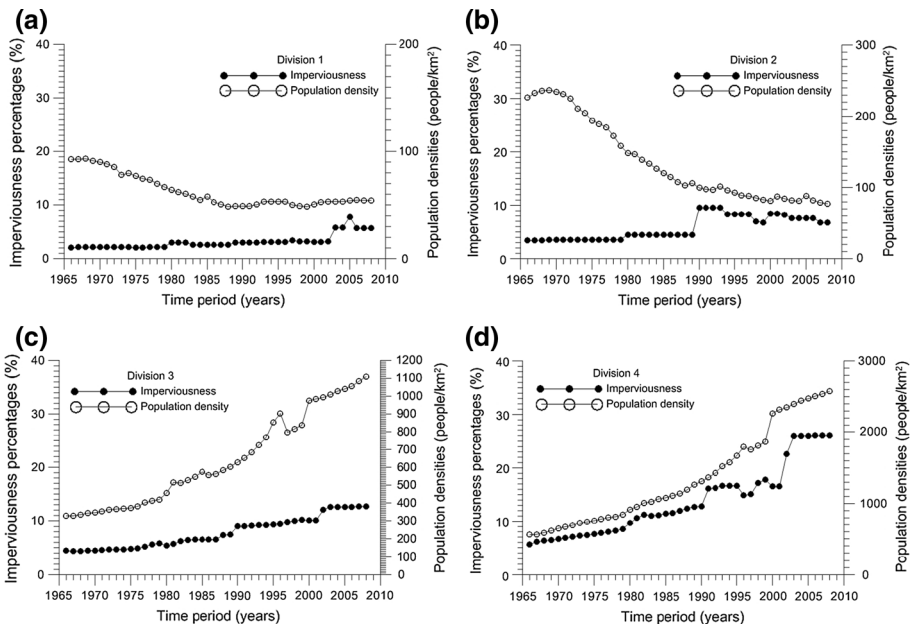


Fig. 3 Changes of population density and imperviousness percentage on the watershed divisions

of rainfall is a time function of period t , isotropy, and a time mean form with nonzero and T time intervals. Rainfall recordings were obtained from 14 raingauges located along the Tamshui River between 1966 and 2008. The scaled climatological mean semivariogram and its power form applied for fitting were calculated as follows:

$$\gamma_d^*(h_{ij}, a) = \omega_0 h^a = 0.093 h^{0.243}, \quad R^2 = 0.906 \quad (16)$$

where ω_0 denotes the scaled climatological mean semivariogram (mm^2).

The hourly variance $s^2(t)$ of each period t can be calculated using hourly measurements of rainfall occurring in the same periods. According to Eqs. (5) and (16), each hourly semivariogram of rainfall is directly calculated from the hourly variance and the scaled climatological mean semivariogram. The estimated area must be divided into M grids before calculating the hourly mean rainfall during storm events over the watershed by applying Eq. (3). The four estimated areas were divided into 1095, 1,748, 2,267, and $1,175 \times 500\text{-m}^2$ grids, respectively (Fig. 2c). This study uses observations from three raingauges located in the Wu-Tu watershed (Jui-Fang, Wu-Tu, and Huo-Shao-Liao) to estimate the hourly mean rainfall.

Hourly effective rainfall defines the difference in rainfall between mean rainfall and its rainfall loss at each time period. Therefore, hourly loss computation is the second job using the constant percentage method before parameter calibration. The constant percentage method defines the losses to be proportional to the rainfall intensity for forcing the shapes of the effective rainfall distribution to be the shape of total rainfall distribution. The available data are only for discharge recording of the watershed outlet. No hydrograph recording of each division, rainfall losses in each division cannot be directly completed by the above definition. This study assumed that the constant percentage of an event is a spatially fixed value distributed over the entire watershed. The rainfall losses having spatiotemporal variations were represented as the products of the constant value and hourly mean rainfall of the divisions, and then the effective rainfall of events was obtained by the definition. The effective rainfall hyetographs of divisions are spatial and temporal inputs to the model for the event-based calibration.

5.2 Calibration with suitable parameter bounds

The model used in this study employs conceptual storage and a storage-routing procedure to route excess rainfall over the watershed divisions and is parallel linked to the watershed outlet. The trends in calibrated storage constants, k_o and k_c , must can actually reflect overland and channel storage effects; particularly, the proportion of excess rainfall as temporary storage in channel or overland flow of the watershed divisions. The model parameters of each division were obtained from 50 samples taken from 102 available rainfall-runoff events between 1966 and 2008. These parameters have their respective physical significances and are combined consequences resulting from hydrological and geomorphic effects of storm events occurred in that time. Therefore, these storage values have their ultimate values and should be appropriately limited in calibration. The lower bounds of storage parameters are certainly zero values, but the upper bounds are hard to be determined directly.

This study determined upper bounds of storage parameters using the following approach: (a) setting up each upper bound of two storage types (overland and channel) and calibrating storage values of all available events using the shuffled complex evolution (SCE) algorithm (Duan et al. 1993); (b) checking separately whether the calibrated values of two storage types are equal to respective upper bounds. If they are not equal, the current upper bounds are largest values of each storage type, should not be increased again; if they are equal, the upper bounds should be increased for recalibration and following step (b); (c) repeating steps (a) and (b) until calibrated storage values of two types for all cases are

not equal, but close to each upper bound. This study considered upper bounds of each watershed divisions to be the same, with two upper bounds for overland storage and channel storage. Table 1 shows a comparison of simulated and observed runoff hydrographs for the four criteria (CE , EQ_p , ET_p , and VER) resulting from the calibration.

As shown in Table 1, considering CE in the calibration, 24 of the 50 rainfall-runoff events produced values exceeding 0.9, whereas 24 events produced values between 0.8 and 0.9, and only two storm events, (1968-07-25) and (2001-06-07), produced values below 0.8. For EQ_p , 22 cases demonstrated less than 20 %, 18 cases ranged between 20 and 30 %, and another ten cases were larger than 30 %. For ET_p , the values for all of the events were below 3 h, except for one event (a storm on 2000-04-23). Only one case (storm, 2004-09-09) was slightly larger than the VER criterion of 10 %.

5.3 Evaluating applicable parameters from two calibrations

One work of the study is to clarify the importance of the calibration work with suitable bounds. Large values for upper bounds were setup in another calibration using the same 50 events and compared their results with previous calibration results. Table 2 lists comparisons between calibration modeling with and without appropriate upper bounds. Figures 4 and 5 show plots for two cases derived from the 50 calibrated events with and without appropriate upper bounds in the two calibrations. Figures 4 and 5 show little differences in the hydrographs between the two calibration simulations. Table 2 also has the same comparison results for three evaluation criteria (CE , EQ_p , and VER) as Figs. 4 and 5, but shows a slight but obvious difference in the ET_p criterion. The calibration with appropriate bounds produces more zero values for the ET_p criterion than that without those does. However, the two calibration results with and without appropriate bounds reveal no obvious differences on four evaluation criteria and hydrograph simulations. Evaluating which calibration is superior seems is difficult given these results (Table 2; Figs. 4, 5). This study further compared the calibrated values of two storage types of four divisions resulting from with and without appropriate bounds, which the overland parameters are plotted in Fig. 6, and the channel parameters are shown in Fig. 7. These two figures show similar storage estimations of numerous cases occurring in the two calibrations; however, a few storage values clearly diverge.

Figure 6 shows the ranges of overland points, which are the concentrated and approximate values between the two calibrations. The overland parameter values of upstream Divisions 1 and 2 mostly centralize on a range smaller than a value of 5; the overland coefficients of Division 3 primarily ranges between an interval of 2 and 7; and those of Division 4 have a wide distribution between 4 and 20. These results indicate that the overland storage of the downstream division has a wider variation range than that of the upstream division has. Similar to the storage values of the overland flow that occurs in watershed divisions, Fig. 7 shows channel storage of the downstream area is also more extensively varied than that of the upstream area. The channel storage variation in Division 4 was primary within 1 and 6; a distribution from 1 to 5 was observed for Division 3; the variation on Division 2 ranged between 0 and 4; and the primary range was smaller than 3 for Division 1.

The model used in this study employs conceptual storages and a storage-routing procedure to route excess rainfall over the watershed divisions and is parallel linked to the watershed outlet. The trends in storage constants, k_o and k_c , reflect overland and channel storage effects in the watershed divisions. Particularly, the proportion of excess rainfall as temporary storage in channel or overland flow depends on the characteristics of the

Table 1 Evaluation criteria the selected events in calibration with appropriate bounds

Event names (times)	Evaluation criteria				Event names (times)	Evaluation criteria			
	CE	EQ _p (%)	ET _p (h)	VER (%)		CE	EQ _p (%)	ET _p (h)	VER (%)
Alice (1966-09-02)	0.82	-26.90	1	-3.81	Storm (1994-06-18)	0.88	-26.41	1	-4.33
Storm (1968-07-25)	0.78	-14.47	1	-2.60	Doug (1994-08-07)	0.82	-38.90	1	-1.30
Elsie (1969-09-26)	0.88	-22.04	0	-2.77	Fred (1994-08-20)	0.95	-18.09	1	-2.64
Jean (1974-07-19)	0.93	-20.82	0	-5.68	Seth (1994-10-09)	0.82	-33.71	2	-3.09
Storm (1974-10-19)	0.95	-11.08	0	-3.47	Zeb (1998-10-15)	0.96	-8.45	0	-2.38
Storm (1976-07-03)	0.83	-12.15	3	-3.95	Storm (1998-11-26)	0.97	-8.87	3	-0.99
Storm (1976-08-11)	0.90	-28.17	1	-2.19	Storm (2000-04-23)	0.83	-33.28	4	-1.08
Norris (1980-08-27)	0.84	-31.34	0	-3.77	Storm (2000-06-17)	0.92	-14.46	-1	-4.85
Storm (1980-11-19)	0.88	-31.55	-1	-5.51	Storm (2000-10-17)	0.91	-21.51	0	1.96
Storm (1984-06-02)	0.89	-32.58	0	-3.85	Bebinc (2000-11-08)	0.90	-17.90	1	3.10
Freda (1984-08-07)	0.84	-34.11	0	-3.73	Storm (2000-12-13)	0.98	-8.98	0	-0.77
Storm (1985-02-08)	0.88	-25.54	0	-0.47	Storm (2000-12-19)	0.91	-16.07	2	-0.37
Nelson (1985-08-22)	0.89	-30.69	0	-1.41	Storm (2001-06-07)	0.73	-22.32	2	-6.91
Brenda (1985-10-03)	0.90	-32.57	0	-1.95	Storm (2001-09-03)	0.88	-29.42	0	-2.63
Wayne (1986-08-22)	0.83	-22.82	1	-4.21	Nari (2001-09-15)	0.95	-15.42	0	-1.16
Alex (1987-07-27)	0.92	-23.93	0	-5.95	Storm (2004-03-26)	0.97	-9.55	0	-0.86
Gerald (1987-09-09)	0.97	4.82	-2	-0.92	Ranani (2004-08-12)	0.92	-23.44	0	-5.62
Lynn (1987-10-23)	0.82	-20.89	-2	-3.44	Storm (2004-09-09)	0.84	-16.86	0	-10.15
Storm (1988-09-16)	0.85	-17.05	1	-3.89	Haima (2004-09-10)	0.97	-10.35	0	-1.14
Storm (1988-09-24)	0.92	-16.82	0	-1.29	Storm (2004-10-18)	0.85	-33.39	2	5.15
Storm (1988-09-28)	0.93	-18.09	2	-0.11	Nannad (2004-12-02)	0.88	-28.67	0	-2.47
Sarah (1989-09-11)	0.86	-26.04	0	-1.45	Storm (2005-10-06)	0.94	2.64	0	-1.90
Storm (1990-09-01)	0.96	-13.15	0	-3.55	Storm (2008-05-30)	0.95	-9.04	1	1.31
Storm (1990-09-03)	0.87	-29.40	1	-3.94	Storm (2008-10-06)	0.89	-27.92	1	1.20
Ruth (1991-10-28)	0.86	-26.99	1	1.58	Storm (2008-10-10)	0.96	-16.02	0	-2.99

watershed divisions. The appropriate bounds are essential to calibration modeling for obtaining applicable parameter values. Otherwise, using inappropriate bounds in a calibration may produce overly large storage values, as in upstream Division 1 (Fig. 6a); also may produce overly small values, as in the downstream division shown (Fig. 6d); may overestimate the parameter values for the channel storages, as in the upstream Division 1 (Fig. 7a).

This study confirmed that storage coefficients should be appropriately restricted to their ultimate bounds in a calibration modeling. Appropriate upper bounds can effectively avoid overly large calibrated values on an upstream area or overly small values on a downstream area. The ultimate bound of the overland storage varied more widely compared with those of the channel storage in the same watershed division. The ultimate bounds of the storage coefficients of the upstream area were less than those of the downstream area. The model calibration with appropriate bounds demonstrated that the storage parameters can adequately represented the watershed situation during urbanization.

5.4 Parameter changes from corresponding imperviousness

Storage coefficients represented the combined effects of the geomorphic and hydrological characteristics derived from a storm event occurred in that time. The geomorphic characteristics are imperviousness, slope, area and stream length etc., while hydrological characteristics are weather factors, antecedent moisture, precipitation, or other unknown variables. Thus, storage values may have disorder variations, but varied in their specific scopes themselves because of hydrological uncertainties. Such uncertainties frequently cause irregular and unpredictable variations in these model parameters, thus necessitating a valid method for examining obvious or visible tendencies toward imperviousness changes. This study used the optimal interval method (Huang et al. 2008a, 2012) to consider the various values of the calibrated parameters in each interval as a fixed value; thus, an identical computation was used for each interval. The optimal magnitude of the interval was finally determined until the first appearance of an obvious tendency between the parameter averages and imperviousness percentages.

Figure 3 shows that imperviousness change has the same tendency as population change on the downstream divisions, whereas imperviousness reversely varies with population change on the upstream divisions. This result reveals that the population change is not in full agreement with the imperviousness change on all of the watershed divisions. Therefore, this study related applicable storages, which derived from the calibration with appropriate bounds, to the corresponding imperviousness percentages. The averages of the storage parameters of two types and imperviousness percentages using the optimal interval method were plotted in Figs. 8a–d for four divisions.

Figure 8 reveals that the applicability of the storage values of two types related to various degrees of urbanization changes. The area of overland storage in a watershed or division is substantially larger than that of channel storage. Regarding the area contributing to outlet runoff, the overland storage must be larger than that of channel storage, with a large difference between the areas of two different storage types. Figures 6 and 7 also show that overland storage varies more widely than channel storage in the same watershed divisions. Therefore, the storage values representing channel storage vary more consistently than the values describing overland storage, which is independent of imperviousness changes. The overland storage k_o varies considerably compared with channel storage k_c , in response to imperviousness, as shown in Figs. 8c, d. Therefore, this study confirmed that

Table 2 Comparisons of the evaluation criteria in calibrations with and without appropriate upper bounds

CE criterion			EQ _p criterion (%)			ET _p criterion (h)			VER criterion (%)		
Intervals	with	without	Intervals	with	without	Intervals	with	without	Intervals	with	without
≥0.9	24	24	≤±10	7	8	0	25	19	≤±5	43	41
0.8–0.9	24	24	±10–20	15	14	±1	15	21	±5–10	6	9
0.7–0.8	2	2	±20–30	18	18	±2	7	7	±10–15	1	0
0.6–0.7	0	0	±30–40	10	10	±3	2	2	±15–20	0	0
< 0.6	0	0	>±40	0	0	±4	1	1	>±20	0	0

overland storage variation was more sensitive to urbanization processes among the four watershed divisions than channel storage was.

Owing to overland storage displayed greater sensitivity compared with channel storage, the imperviousness was as a primary variable of the overland storage and considered the channel storage k_c was each constant across each division. This study separately averaged channel storages of each divisions calibrated from the calibration with appropriate bounds to obtain the respective division channel constants. Table 3 shows the averaged channel constants of each watershed division. These constant values denoted the channel storages of the divisions and were more independent than the overland storage during the urbanization process. Furthermore, this study used regression analysis to correlate the discrete values of overland storages k_o with the corresponding imperviousness percentages. The power equations (natural logarithm) of each division for further study are expressed as follows:

$$k_{o1} = 5.96Im_1^{-0.23}, \quad R^2 = 0.98 \tag{17}$$

$$k_{o2} = 3.84Im_2^{-0.24}, \quad R^2 = 0.76 \tag{18}$$

$$k_{o3} = 13.50Im_3^{-0.50}, \quad R^2 = 0.61 \tag{19}$$

$$k_{o4} = 34.05Im_4^{-0.30}, \quad R^2 = 0.72 \tag{20}$$

where k_{oi} denotes the overland storage of the i -th watershed division and Im_i is the i -th impervious percentage of the i -th divisions. These equations show the continuous relationships of four watershed divisions for changes in the overland storages related to changes in the corresponding imperviousness percentages. Their coefficients of determination (R^2) reveal that these evaluated relationships are favorable. The correlations in Equations (17)–(20) provide conveniently available data for exploring continuous changes in the overland storage k_o that occurred in response to continuous changes in the imperviousness.

5.5 Verifying the relationships between overland storages and imperviousness

The overland storage was more sensitive to changes in the imperviousness than the channel storage was. Therefore, the overland storages of each division were separately related to the division imperviousness, and channel storages were viewed as each constant for four divisions. Following work is to verify the reported correlations between the overland storages k_o and the imperviousness percentages. The data on 52 rainfall-runoff events from 2002 to 2008 were used to examine these correlations for further applications. Similar to

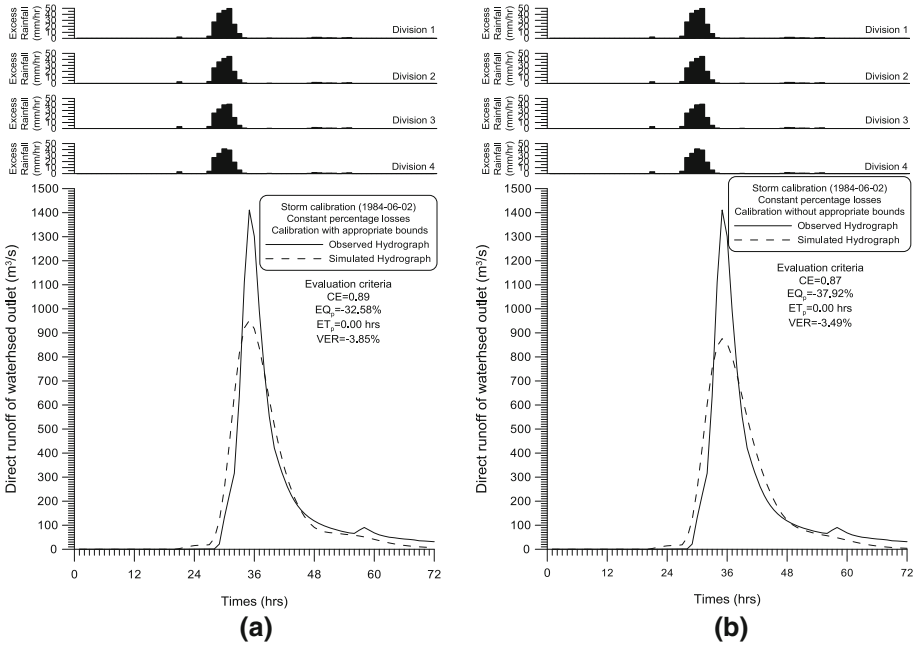


Fig. 4 Simulation comparisons of a storm event resulting from two calibrations with and without appropriate bounds

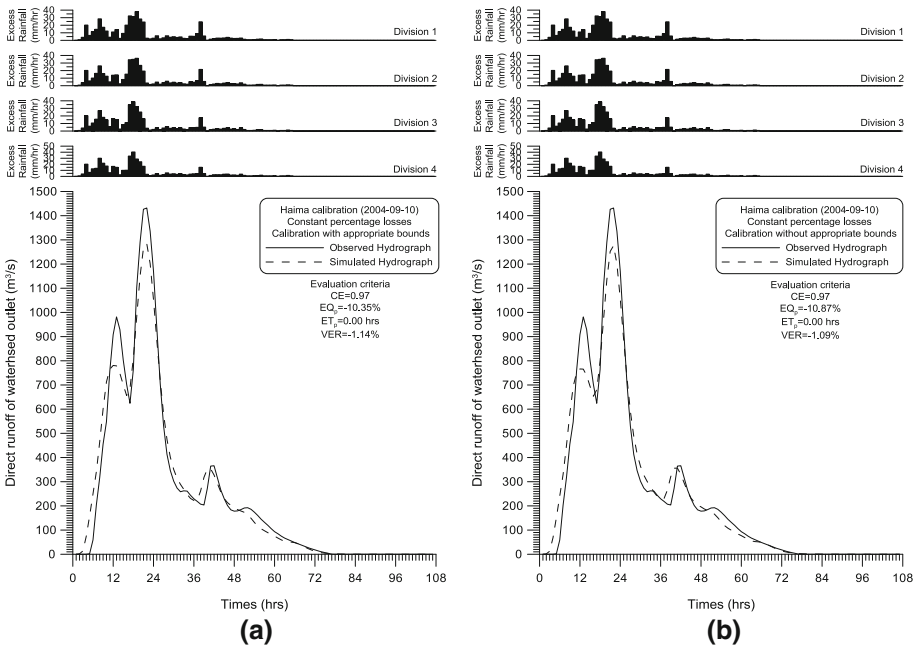


Fig. 5 Simulation comparisons of a typhoon Haima resulting from two calibrations with and without appropriate bounds

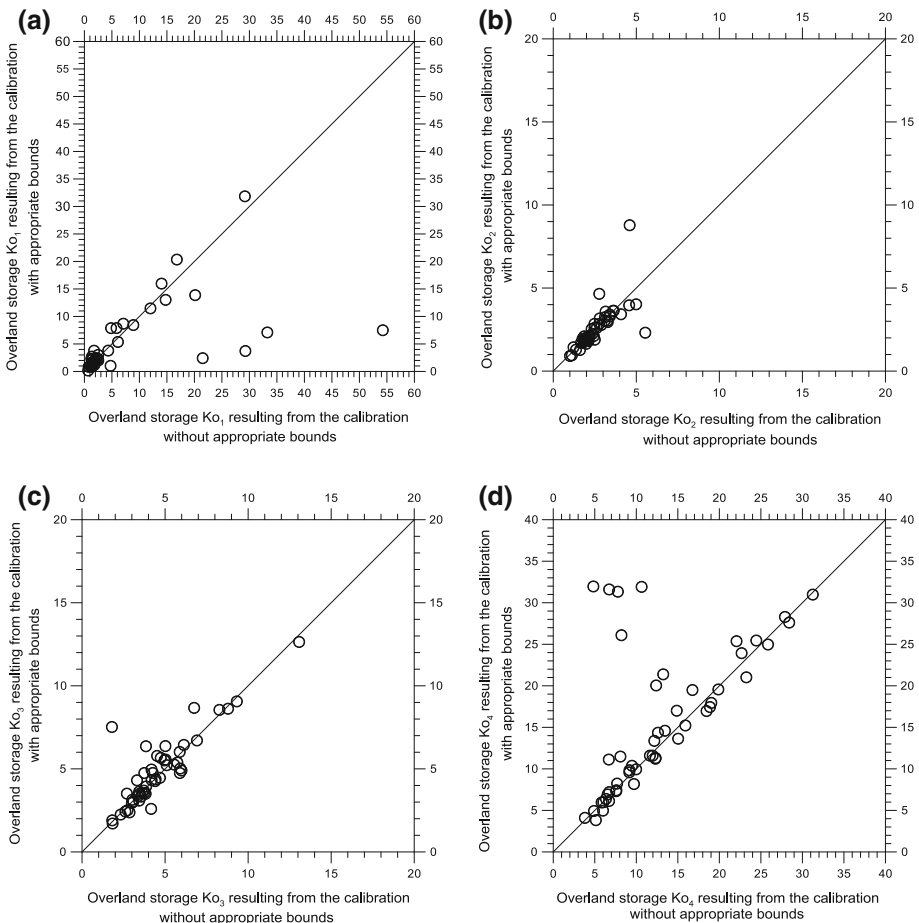


Fig. 6 Overland storages of four divisions based on two calibrations with and without appropriate bounds

the methods previously used, mean rainfall, constant ratios of losses, and their loss values of hourly based events were completed using the Kriging and the constant percentage methods. These products were subtracted from division mean rainfall to yield effective rainfall hietographs of each division, which allowed the rainfall-runoff model to be verified. The channel storages k_c were constants, as shown in Table 3. The overland storages of each division k_o were determined using the correlations of each division, as expressed by Eqs. (17–20), i.e., overland storage k_o varied nonlinearly with changes in the imperviousness percentages. The effective rainfall, constants k_c , and varying k_o of each division were subsequently used to produce outlet hydrographs which were compared with their observed hydrographs using the same evaluation criteria.

Table 4 shows the comparison results among the 52 cases, and Fig. 9 shows the plots of the two verified cases among the 52 rainfall-runoff events. Regarding the CE for model verification, 30 calibrated events equaled or exceeded 0.8, 19 cases were within the interval of 0.7–0.8, and the other eight were smaller than the value of 0.7. Regarding EQ_p , 31 cases produce less than 20 %, eight cases produced values that ranged between 20 and 30 % and that of the others 13 cases were larger than 30 %. The ET_p values were all less than or

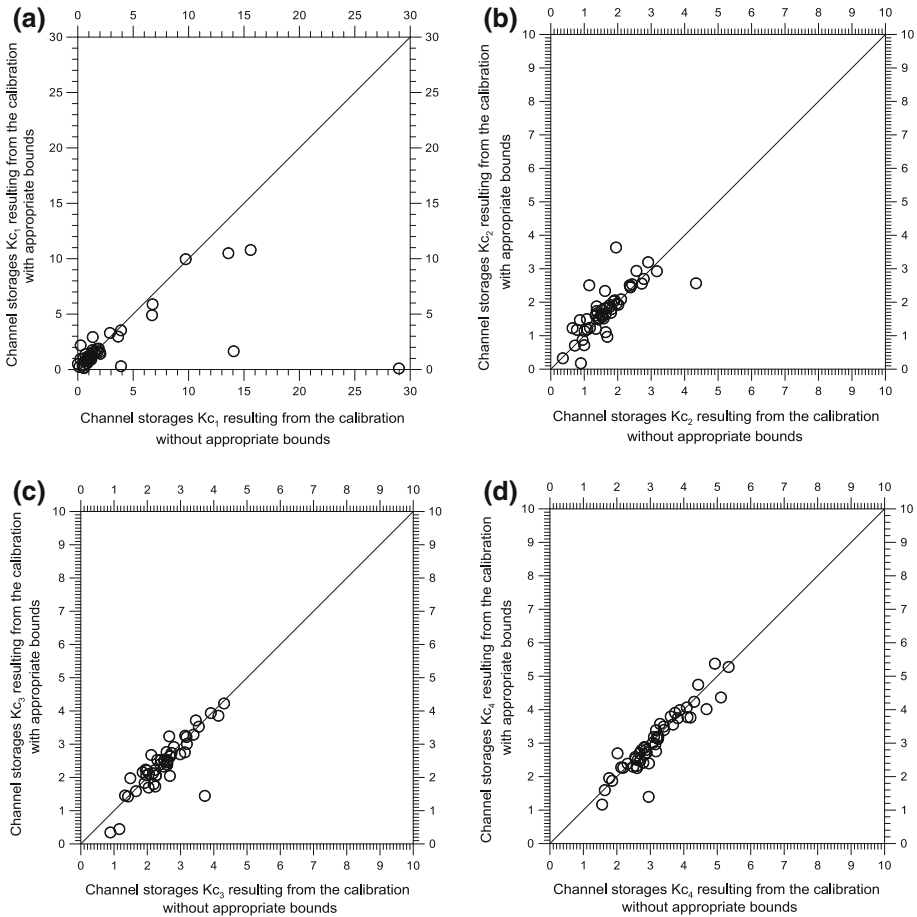


Fig. 7 Channel storages of four divisions based on two calibrations with and without appropriate bounds

equal to 3 h; only one values exceeded 3 h. The VER values of all the examined events were less than 10 %, but one slightly exceeded 10 %.

The coefficient of determination (R^2) based on regression equations clearly exhibited nonlinear correlations between the overland k_o and the imperviousness of each division. The verification results based on 52 cases for changes in overland storage related to changes in imperviousness also indicated favorable correlations. These correlations were confirmed that the Eqs. (17–20) can appropriately reflected changes in the overland storages resulting from change in the imperviousness. The imperviousness is thus a primary variable that can be applied to evaluate changes in hydrograph characteristics during urbanization developments in the Wu-Tu watershed divisions.

5.6 Changes in hydrograph characteristics on watershed divisions

The watershed response to rainfall input is considered to represent a transformation between effective rainfall and direct runoff. This transformation is also referred to as an IUH, which represents the hydrological status of an area. This study used a semidistributed

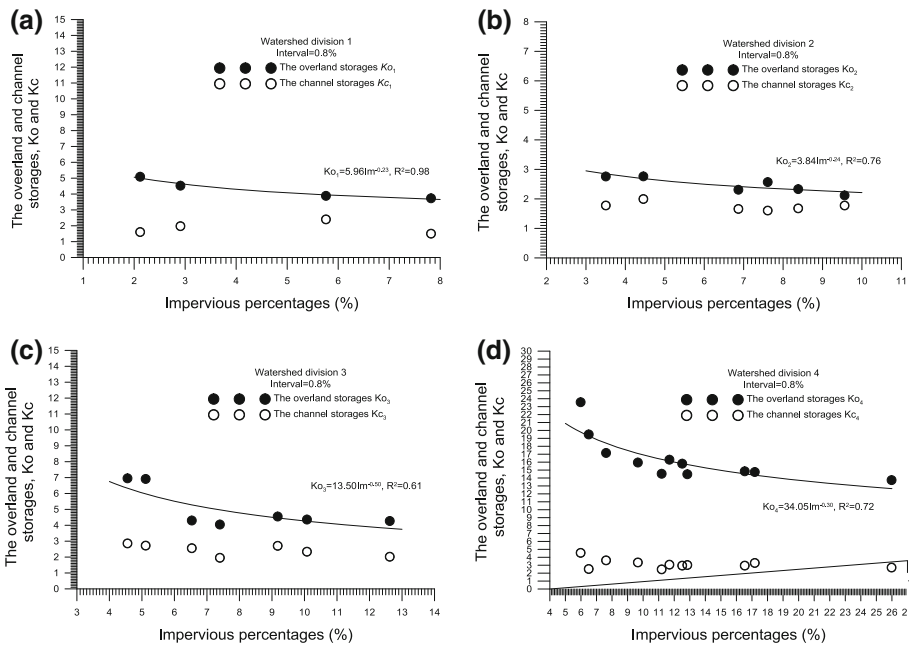


Fig. 8 Relations between storage parameters and impervious percentages of the four watershed divisions

Table 3 Averaged constants for channel storages of four watershed divisions

Watershed divisions	Channel storages k_c
1	1.979
2	1.785
3	2.427
4	3.057

model having four flow paths by dividing the watershed into four divisions. These flow paths were represented by the IUHs containing storages of two types, overland and channel storages. The overland storage k_o varied considerably because it was sensitive to the imperviousness, whereas the channel storage k_c was irrelevant to the imperviousness. The four nonlinear correlations of four divisions between the overland storage and imperviousness have been identified as specific power forms. Storage values of the model can be thus obtained using the given imperviousness changes representing various degrees of urbanization processes. Predetermining storage values of two types of each division enable to discuss each change in the division IUHs and their shape characteristics during urbanization changes.

In order to understand changes of rural to urban areas in IUH characteristics, the study considered the minimal and maximal imperviousness percentages of an area, respectively. Table 5 lists these changes in IUH characteristics between the rural and urban status of the four divisions. The analytical results indicated that the IUH shapes across divisions became more pronounced, with a forward shift in the peak, when imperviousness increased.

Table 4 Evaluation criteria of the selected events in verification

Event names (times)	Evaluation criteria				Event names (times)	Evaluation criteria			
	CE	EQ _p (%)	ET _p (h)	VER (%)		CE	EQ _p (%)	ET _p (h)	VER (%)
Elaine (1968-09-28)	0.75	-16.13	0	-0.04	Storm (2005-02-24)	0.62	-5.44	1	0.03
Fran (1970-09-05)	0.87	-23.66	-1	-0.99	Storm (2005-05-09)	0.60	-11.70	0	-1.19
Agnes (1971-09-17)	0.74	-26.84	2	-0.57	Storm (2005-05-29)	0.77	-3.39	0	-2.06
Bess (1971-09-22)	0.75	-35.89	3	-1.26	Haitang (2005-07-17)	0.81	9.18	3	0.46
Betty (1975-09-22)	0.62	-32.61	0	-1.05	Talim (2005-08-30)	0.87	15.98	0	2.14
Storm (1976-09-16)	0.72	-30.35	0	-1.30	Longwang (2005-10-01)	0.85	-25.39	1	-1.98
Storm (1977-11-14)	0.91	-21.95	0	3.07	Storm (2005-12-11)	0.80	-11.32	1	7.34
Ora (1978-10-12)	0.83	-34.31	3	-5.36	Storm (2006-01-20)	0.89	-3.59	-1	2.76
Andy (1982-07-29)	0.82	-35.56	0	-10.65	Storm (2006-04-26)	0.60	5.19	2	0.81
Celcil (1982-08-10)	0.70	-34.07	2	-4.89	Chanchu (2006-05-13)	0.82	-7.53	3	0.71
Storm (1984-11-18)	0.76	-32.01	1	-4.06	Storm (2006-05-29)	0.77	-19.53	2	0.93
Jeff (1985-07-29)	0.94	-17.03	-2	1.21	Storm (2006-06-08)	0.87	-15.46	2	-0.13
Storm (1989-07-28)	0.88	-17.27	-2	-2.40	Storm (2006-09-08)	0.79	-34.90	3	0.71
Polly (1992-08-27)	0.72	-34.57	-1	-0.85	Storm (2006-12-13)	0.80	-10.11	-1	1.27
Storm (1993-06-05)	0.78	17.04	3	-0.10	Storm (2006-12-18)	0.70	-22.58	0	4.70
Gladys (1994-09-01)	0.88	-20.44	0	-0.53	Storm (2007-03-06)	0.85	-23.69	-1	1.12
Zane (1996-09-27)	0.82	-32.42	1	-1.23	Storm (2007-06-15)	0.86	-11.23	1	6.98
Dan (1999-10-03)	0.87	11.03	2	-1.21	Storm (2007-06-26)	0.75	12.33	0	-0.04
Storm (2000-06-12)	0.72	-3.40	-3	0.69	Wutip (2007-08-07)	0.61	-37.07	3	-1.71
Kai-tak (2000-07-08)	0.81	-32.74	1	0.01	Storm (2007-09-04)	0.80	-25.45	2	2.83
Storm (2000-11-04)	0.82	-1.04	-2	-2.33	Storm (2007-11-04)	0.93	-10.59	3	4.63
Storm (2000-11-16)	0.88	-1.85	1	3.38	Mitag (2007-11-18)	0.89	-32.25	3	0.64
Storm (2001-09-05)	0.87	-4.38	3	3.09	Storm (2008-01-21)	0.67	-11.12	-4	0.55
Rammasun (2002-07-03)	0.82	-10.16	1	-1.72	Storm (2008-02-17)	0.76	0.53	-1	2.12
Storm (2004-07-08)	0.76	-9.48	0	-2.24	Jangmi (2008-09-28)	0.89	-9.48	3	-2.40
Storm (2004-12-23)	0.75	-1.06	0	1.45	Storm (2008-12-08)	0.72	-13.33	0	-2.15

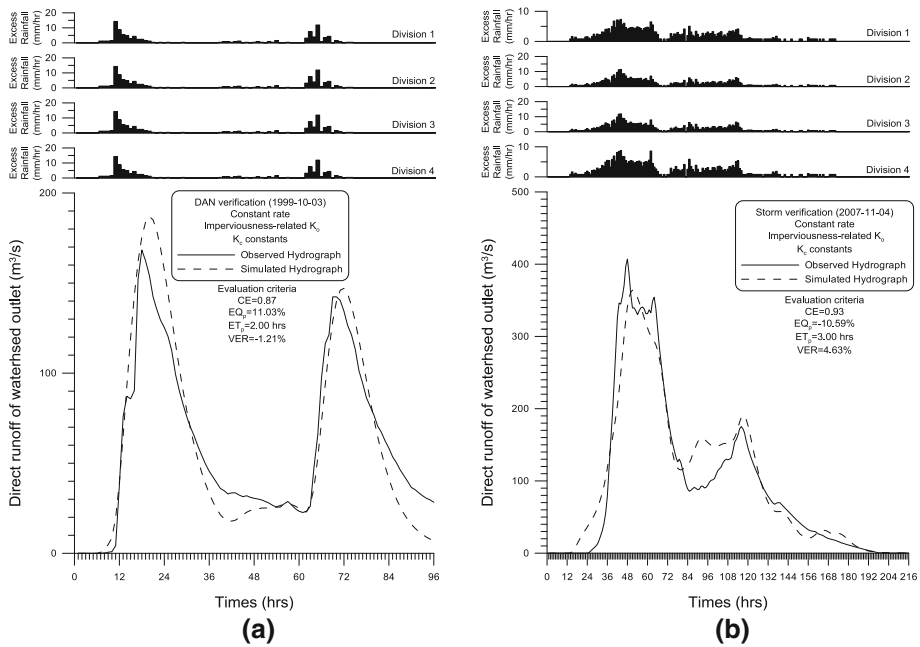


Fig. 9 Verifications of urbanization linkages using observed and simulated hydrographs of typhoons and storms

Table 5 Changes in IUH characteristics from rural to urban areas on four watershed divisions

Watershed divisions	Changes in hydrographs from imperviousness changes			
	Time to peak (h)		Peak discharge (m ³ /s)	
	Rural ^a	Urban ^b	Rural	Urban
Division 1	11.97	11.66	5.291	5.585
Division 2	7.64	7.20	13.813	14.734
Division 3	7.79	6.85	12.504	15.513
Division 4	7.01	6.14	3.347	4.455

^a Rural denotes minimum imperviousness percentages of divisions between 1966 and 2008

^b Urban represents maximum imperviousness percentages of divisions between 1966 and 2008

Table 5 also shows the characteristic changes in IUHs across watershed divisions. Because a rural area was changed into an urban area, the times in which the hydrograph peaks occurred in Divisions 1-4 reduced from 11.97 to 11.66 h, 7.64 to 7.20 h, 7.79 to 6.85 h, and 7.01 to 6.14 h, respectively. The peak discharges changed as follows: 5.291–5.585 m³/s in Division 1; 13.813–14.734 m³/s in Division 2; 12.504–15.513 m³/s in Division 3; and 3.347–4.455 m³/s in Division 4.

An increase in the imperviousness over an area is typically caused by an increase in population concentration and the demands of urban lift. By contrast, population moves from an area causes an uncertain decrease in imperviousness. However, imperviousness

changes are a direct factor affecting the hydrological features of a region. Table 5 shows that an increase in the imperviousness reduced the time to peak and increased the peak discharge of the hydrograph on an area outlet. Furthermore, urbanization behavior and its effects are nonuniformly distributed over a watershed, as evidenced in Fig. 3 and Table 5. Small changes in imperviousness on the upstream Divisions 1 and 2 resulted in minor alterations in the hydrograph characteristics. By contrast, marked urbanization in downstream Divisions 3 and 4 caused a large alteration in the time to peak of up to 10 % and caused peak discharges that exceeded 20 times that of the original or natural status to occur.

6 Conclusions

This study discussed the changes in storage coefficients of two types responded from change in the imperviousness for linking them with correlations and evaluated changes of rural to urban areas in shape characteristics of the division IUHs. The methods used in this study include the block Kriging method, the constant percentage method, the semidistributed model with parallel connections, optimal interval, and regression analysis combined with a natural logarithm. The study also emphasize a determination of suitable parameter bounds should be attached importance to a calibration process. Completing the goal of this study using these methods did not require detailed hydrological data, only based on 50 calibrated and 52 verified events, and imperviousness data.

Hydrograph simulations, four evaluation criteria, and the calibrated storage coefficients were compared between calibrations with and without appropriate bounds. The comparison results indicated: (1) The simulated hydrographs were similar to the observed hydrographs produced by the same events; (2) No large differences between three evaluation criteria (CE, EQ_p, and VER), but only a slight divergence from the ET_p criterion; (3) Approximate storage values of most cases occurring in the two calibrations, but a few have obvious diverges. The third comparison shows that inappropriate bounds in a calibration may produce nonsignificant storage values, which may be overly large or overly small in upstream or downstream areas. A calibration with appropriate bounds can effectively determine applicable storage coefficients for indeed relating them to the imperviousness. The storage representing overland feature indicates a more noticeable change than the storage denoting channel meaning does in the presence of related storage coefficient changes with imperviousness changes. The channel storage is independent of the urbanization process and as constants for each division. The regression analysis with a power form provides a method for linking continuous relationships between overland storages and the corresponding imperviousness percentages. These verified power equations yielded parameter values representing overland storages of each division based on the observed imperviousness data. Changes in hydrograph characteristics of watershed divisions were identified based on the verified correlations and the given imperviousness. The evaluated hydrograph characteristics during urbanization developments include the time to peak for the time characteristic and the peak discharge for the flow characteristic.

Regarding the shape characteristics of division IUHs in the rural and urban areas, the decreased rates of the times to peak were approximately -2.59 , -5.76 , -12.07 , and -12.41 % of Divisions 1–4, respectively. The increased rates of the peak discharges were approximately 5.56, 6.67, 24.06, and 33.10 % of the upstream to downstream divisions, respectively. Increased imperviousness caused a decrease in the time to peak and an increase in the peak discharge for the IUH of an area. Furthermore, the varied urbanization

effects across watershed divisions were nonuniform spatial changes because of various imperviousness changes on Divisions 1–4. Large changes in imperviousness on the downstream divisions marked urbanization resulted in reduced the time characteristic of IUH by at least 10 % regarding the time to peak, and the flow characteristics exceeded an increment of 20–30 % regarding peak discharge. The analysis results indicated that hydrograph characteristics of the watershed divisions inevitably changed with urbanization. A large change in imperviousness might be linked to an increased incidence of disasters.

References

- Agirre U, Goñi M, López JJ, Gimena FN (2005) Application of a unit hydrograph based on subwatershed division and comparison with Nash's instantaneous unit hydrograph. *Catena* 64:321–332
- Ahmad MM, Ghumman AR, Ahmad S (2009) Estimation of Clark's instantaneous unit hydrograph parameters and development of direct surface runoff hydrograph. *Water Resour Manag* 23:2417–2435
- Arnell V (1982) Estimating runoff volumes from urban areas. *Water Resour Bull* 18:383–387
- Aronica G, Cannarozzo M (2000) Studying the hydrological response of urban catchments using a semi-distributed linear non-linear model. *J Hydrol* 238:35–43
- Barron OV, Donn MJ, Barr AD (2013) Urbanisation and shallow groundwater: predicting changes in catchment hydrological responses. *Water Resour Manag* 27:95–115
- Basistha A, Arya DS, Goel NK (2008) Spatial distribution of rainfall in Indian himalayas: a case study of Uttarakhand region. *Water Resour Manag* 22:1325–1346
- Bastin G, Lorent B, Duque C, Gevers M (1984) Optimal estimation of the average rainfall and optimal selection of raingauge locations. *Water Resour Res* 20:463–470
- Bonta JV, Amerman CR, Harlukowicz TJ, Dick WA (1997) Impact of coal surface mining on three Ohio watersheds-surface-water hydrology. *J Am Water Resour As* 33:907–917
- Cheng SJ (2010a) Generation of runoff components based on serial exponential reservoirs. *Water Resour Manag* 24:3561–3590
- Cheng SJ (2010b) Hydrograph characteristics of quick and slow runoffs of a watershed outlet, Taiwan. *Hydrol Process* 24:2851–2870
- Cheng SJ (2010c) Inferring hydrograph components from rainfall and streamflow records using a Kriging method-based linear cascade reservoir model. *J Am Water Resour As* 46:1171–1191
- Cheng SJ (2011a) Raingauge significance evaluation based on mean hyetographs. *Nat Hazards* 56:767–784
- Cheng SJ (2011b) The best relationship between lumped parameters and urbanized factors. *Nat Hazards* 56:853–867
- Cheng SJ, Wang RY (2002) An approach for evaluating the hydrological effects of urbanization and its application. *Hydrol Process* 16:1403–1418
- Cheng SJ, Hsieh HH, Wang YM (2007) Geostatistical interpolation of space–time rainfall on Tamshui River Basin, Taiwan. *Hydrol Process* 21:3136–3145
- Cheng KS, Lin YC, Liou JJ (2008a) Rain-gauge network evaluation and augmentation using geostatistics. *Hydrol Process* 22:2554–2564
- Cheng SJ, Hsieh HH, Lee CF, Wang YM (2008b) The storage potential of different surface coverings for various scale storms on Wu-Tu watershed, Taiwan. *Nat Hazards* 44:129–146
- Cheng SJ, Lee CF, Lee JH (2010) Effects of urbanization factors on model parameters. *Water Resour Manag* 24:775–794
- Cheng CD, Cheng SJ, Wen JC, Lee JH (2012) Effects of raingauge distribution on estimation accuracy of areal rainfall. *Water Resour Manag* 26:1–20
- Cheng CD, Cheng SJ, Wen JC, Lee JH (2013) Time and flow characteristics of component hydrographs related to rainfall-streamflow observations. *J Hydrol Eng* 18:675–688
- Clarke RT (1973) A review of some mathematical models used in hydrology, with observations on their calibration and use. *J Hydrol* 19:1–20
- Duan Q, Gupta VK, Sorooshian S (1993) Shuffled complex evolution approach for effective and efficient global minimization. *J Optim Theory Appl* 76:501–521
- Goovaerts P (2000) Geostatistical approaches for incorporating elevation into the spatial interpolation of rainfall. *J Hydrol* 228:113–129
- Gremillion P, Gonyeau A, Wanielista M (2000) Application of alternative hydrograph separation models to detect changes in flow paths in a watershed undergoing urban development. *Hydrol Process* 14:1485–1501

- Hagg W, Braun LN, Kuhn M, Nesgaard TI (2007) Modelling of hydrological response to climate change in glacierized Central Asian catchments. *J Hydrol* 332:40–53
- Hsieh LS, Wang RY (1999) A semi-distributed parallel-type linear reservoir rainfall-runoff model and its application in Taiwan. *Hydrol Process* 13:1247–1268
- Huang HJ, Cheng SJ, Wen JC, Lee JH (2008a) Effect of growing watershed imperviousness on hydrograph parameters and peak discharge. *Hydrol Process* 22:2075–2085
- Huang SY, Cheng SJ, Wen JC, Lee JH (2008b) Identifying peak-imperviousness-recurrence relationships on a growing-impervious watershed, Taiwan. *J Hydrol* 362:320–336
- Huang SY, Cheng SJ, Wen JC, Lee JH (2012) Identifying hydrograph parameters and their relations to urbanization variables. *Hydrol Sci J* 57:144–161
- Isaaks EH, Srivastava RM (1989) *Applied Geostatistics*. Oxford University Press, New York
- Jakeman AJ, Hornberger GM (1993) How much complexity is warranted in a rainfall-runoff model? *Water Resour Res* 29:2637–2649
- Jakeman AJ, Littlewood IG, Whitehead PG (1990) Computation of the instantaneous unit hydrograph and identifiable component flows with application to two upland catchments. *J Hydrol* 117:275–300
- Junil P, Kang IS, Singh VP (1999) Comparison of simple runoff models used in Korea for small watersheds. *Hydrol Process* 13:1527–1540
- Kang IS, Park JI, Sing VP (1998) Effect of urbanization on runoff characteristics of the On-Cheon stream watershed in Pusan, Korea. *Hydrol Process* 12:351–363
- Kliment Z, Matoušková M (2009) Runoff changes in the Šumava Mountains (Black Forest) and the Foothill Regions: extent of influence by human impact and climate Change. *Water Resour Manag* 23:1813–1834
- Lebel T, Bastin G (1985) Variogram identification by the mean squared interpolation error method with application to hydrologic field. *J Hydrol* 77:31–56
- Lee J, Heaney J (2003) Estimation of urban imperviousness and its impacts on storm water systems. *J Water Resour Plan Manag* 129:419–426
- Legesse D, Vallet-Coulomb C, Gasse F (2003) Hydrological response of a catchment to climate and land use changes in Tropical Africa: case study South Central Ethiopia. *J Hydrol* 275:67–85
- Li YJ, Cheng SJ, Pao TL, Bi YJ (2012) Relating hydrograph components to rainfall and streamflow: a case study from northern Taiwan. *Hydrol Sci J* 57:861–877
- Liu A, Goonetilleke A, Egodawatta P (2012) Inadequacy of land use and impervious area fraction for determining urban stormwater quality. *Water Resour Manag* 26:2259–2265
- Nash JE (1957) The form of the instantaneous unit hydrograph. *IAHS Publications* 45:112–121
- Nash JE, Sutcliffe JV (1970) River flow forecasting through conceptual models: 1. a discussion of principles. *J Hydrol* 10:282–290
- Olivera F, DeFee BB (2007) Urbanization and its effect on runoff in the Whiteoak Bayou watershed, Texas. *J Am Water Resour As* 43:170–182
- Rodriguez F, Andrieu H, Creutin JD (2003) Surface runoff in urban catchments: morphological identification of unit hydrographs from urban databanks. *J Hydrol* 283:146–168
- Simmons DL, Reynolds RJ (1982) Effects of urbanization on base flow of selected South-Shore Streams, Long Island, New York. *Water Resour Bull* 18:797–805
- Singh RB (1998) Land use/cover changes, extreme events and ecohydrological response in the Himalayan region. *Hydrol Process* 12:2043–2055
- Syed KH, Goodrich DC, Myers DE, Sorooshian S (2003) Spatial characteristics of thunderstorm rainfall fields and their relation to runoff. *J Hydrol* 271:1–21
- Xie H, Zhang X, Yu B, Sharif H (2011) Performance evaluation of interpolation methods for incorporating rain gauge measurements into NEXRAD precipitation data: a case study in the Upper Guadalupe River Basin. *Hydrol Process* 25:3711–3720
- Yang X, Liu Z (2005) Use of satellite-derived landscape imperviousness index to characterize urban spatial growth, computers. *Environ Urban Syst* 29:524–540
- Yue S, Hashino M (2000) Unit hydrographs to model quick and slow runoff components of streamflow. *J Hydrol* 227:195–206